Disrupted Topological Organization of the Brain Structural Network in Patients With Thyroid-Associated Ophthalmopathy

Qian Wu,[1] Hao Hu,[1] Wen Chen,[1] Huan-Huan Chen,[2] Lu Chen,[1] Jiang Zhou,[1] Hu Liu,[3] Fei-Yun Wu,[1] and Xiao-Quan Xu[1]

[1]Department of Radiology, The First Affiliated Hospital of Nanjing Medical University, Nanjing, China
[2]Department of Endocrinology, The First Affiliated Hospital of Nanjing Medical University, Nanjing, China
[3]Department of Ophthalmology, The First Affiliated Hospital of Nanjing Medical University, Nanjing, China

Correspondence: Fei-Yun Wu, and Xiao-Quan Xu, Department of Radiology, The First Affiliated Hospital of Nanjing Medical University, No. 300, Guangzhou Road, Gulou District, Nanjing, P.R. China;
wfy_njmu@163.com.

Xiao-Quan Xu, Associated Professor, Department of Radiology, The First Affiliated Hospital of Nanjing Medical University, No. 300, Guangzhou Road, Gulou District, Nanjing, P.R. China;
xiaoquanxu_1987@163.com.

QW, HH, and WC contributed equally to this work.

PURPOSE. Increasing evidence indicated that thyroid-associated ophthalmopathy (TAO) might be a neural related disease more than an ocular disease. In this study, we aimed to investigate the alterations of structural brain connectome in patients with TAO.

METHODS. Twenty-seven patients with TAO and 27 well-matched healthy controls underwent diffusion tensor imaging. Graph theoretical analyses, including global (shortest path length, clustering coefficient, small-worldness, global efficiency, and local efficiency) and nodal (nodal betweenness, nodal degree, and nodal efficiency) topological properties and network-based statistics were performed to evaluate TAO-related changes in brain network pattern. Correlations were assessed between the network properties and clinical variables, including disease duration, visual acuity, neuropsychiatric measurements, and serum thyroid function indexes.

RESULTS. Compared with healthy controls, patients with TAO exhibited preserved global network parameters but altered nodal properties. We found decreased nodal betweenness and nodal degree in right anterior cingulate and paracingulate gyri, decreased nodal degree and nodal efficiency in the right orbital part of middle frontal gyrus (ORBmid), whereas increased nodal degree and nodal efficiency in the left cuneus. Decrease of structural connectivity strength was found involving the right ORBmid, right putamen, left caudate nucleus, and left medial superior frontal gyrus. Significant correlations were also found between nodal properties and neuropsychological performances as well as visual acuity.

CONCLUSIONS. Patients with TAO developed disruption of structural brain network connectome. Disrupted topological organization of the brain structural network may be associated with the clinical-psychiatric dysfunction of patients with TAO.

Keywords: thyroid-associated ophthalmopathy, structural network, diffusion tensor imaging, graph theory

Thyroid-associated ophthalmopathy (TAO) is a multifactorial autoimmune disease that usually presents as exophthalmos, swelling of eyelids, diplopia, and visual impairment.[1,2] Besides the traditionally focused ocular manifestations, patients with TAO also frequently suffer from a series of mental syndromes, ranging from affective dysfunctions (irritability, anxiety, and depression) to cognitive deficits (impairments in memory, attention, concentration, and planning).[3–5] Previously, clinical-psychological studies indicated that these neuropsychological disturbances may be related to impaired visual function, altered facial appearance, or disturbed circulating thyroid hormones.[5–7] However, a considerable part of the patients has been observed to undergo affective symptoms before the onset of ocular symptoms, and even in euthyroid condition.[3,8,9]

Recently, structural neuroimaging approaches have been utilized to explore the underlying neurobiological alterations of TAO.[10,11] One study using voxel-based morphometry and diffusion tensor imaging (DTI) reported decreased grey matter volume combined with decreased fractional anisotropy and increased diffusivities in brain regions that connected with vision and cognition deficits in the TAO cohort.[10] The other study demonstrated localized grey matter thinning corresponding to emotional and cognitive changes of TAO.[11] This evidence showed that TAO was related to both morphological and microstructural changes of the brain, which suggested that it might be a neural-related disease more than an ocular disease. However, these two studies only focused on the changes of individual structures, whereas they ignored the relationships among different structures. The interregional interactions among anatomically separated structures could also play important roles in processing complex neuropsychiatric symptoms.[12,13]

Graph theoretical analysis is a method that quantifies the human brain connectivity as a topological network.[14,15] As the main technique to noninvasively map white matter fiber tracts, DTI serves as a valuable tool to analyze the topological organization of the brain by construction of structural network.[16,17] In the structural connectomics, brain regions are defined as nodes and white matter tracts between them are taken as edges.[14] Hence, disruption of focal brain regions and interregional connections can be reflected by changes of network topological properties. This approach has been widely applied in various mental and psychological disorders and displayed the potency to elucidate underlying neural mechanisms.[18–20] In this view, we hypothesized that the potential alterations of structural brain network of patients with TAO could also be displayed by this application.

In the present study, we used the DTI technique combined with graph theoretical analysis to investigate the characteristic changes of structural network properties in patients with TAO, in order to enhance current understanding about the neural patterns behind the disease.

MATERIALS AND METHODS

Subjects

This study was approved by the institutional review board of the First Affiliated Hospital of Nanjing Medical University. Informed consent was obtained from all participants. Twenty-seven right-handed patients with TAO (19 women and 8 men, mean age 38.5 ± 14.9 years) and 27 healthy controls (HCs; 19 women and 8 men, mean age 38.5 ± 14.5 years) were enrolled. Before magnetic resonance imaging (MRI) scanning, all the patients with TAO had stayed in a hematologically euthyroid state for a period of time (mean 6.3 ± 4.7 months) with a history of antithyroid treatment. All the HCs had no history of dysthyroidism. Participants were excluded if they had eye surgery or other ocular diseases (strabismus, amblyopia, glaucoma, etc.), suffered from psychiatric disorders, or had contraindications of an MRI examination.

Clinical Assessment

Patients with TAO were clinically diagnosed by an experienced endocrinologist and the clinical activity score (CAS) was calculated in accordance with the European Group on Graves' Orbitopathy recommendation.[21] Serum thyroid function and visual acuity examinations were administered to both patients with TAO and HCs.

Psychometric and cognitive assessments were performed for each participant. The Hamilton Depression Rating Scale (HDRS) and the Hamilton Anxiety Rating Scale (HARS) were used to evaluate depressive and anxious symptoms, respectively. Cognitive function was measured using the Mini-Mental State Examination (MMSE). Besides, patients with TAO also underwent a quality of life (QOL) questionnaire, which contains questions on visual functioning and appearance. Detailed demographic and clinical information of our subjects are summarized in Table 1.

MRI Data Acquisition

MRI acquisition was performed with a 3.0 T MR scanner (Magnetom Skyra; Siemens Healthcare, Erlangen, Germany)

TABLE 1. Demographic and Clinical Characteristics of Patients With TAO and Controls

Sample Characteristics	TAO ($n = 27$)	HC ($n = 27$)	_P_ Value
Age, y	38.5 ± 14.9	38.5 ± 14.5	>0.999
Gender, F/M	19 / 8	19 / 8	>0.999
Education, y	12.6 ± 4.4	12.4 ± 4.7	0.881
Disease duration, mo	24.0 ± 39.0	–	
CAS	2.4 ± 1.4	–	
FT3, pmol/L	5.34 ± 1.16	4.92 ± 0.91	0.144
FT4, pmol/L	17.23 ± 3.56	16.76 ± 1.76	0.535
TSH, mIU/L	1.657 ± 1.330	2.148 ± 0.854	0.114
Visual acuity	0.85 ± 0.21	0.96 ± 0.18	0.038
Total score of QOL			
Visual functioning	60.8 ± 30.7	–	
Appearance	57.5 ± 20.7	–	
Total score of HDRS	18.4 ± 7.0	1.9 ± 2.2	<0.001
Total score of HARS	19.7 ± 7.0	2.4 ± 2.5	<0.001
Total score of MMSE	27.7 ± 1.8	29.4 ± 0.9	<0.001

**Note:** Data are presented as means ± standard deviations.

CAS, clinical activity score; FT3, free triiodothyronine (reference value 3.10 – 6.80 pmol/L); FT4, free thyroxine (reference value 12.00 – 22.00 pmol/L); TSH, thyroid-stimulating hormone (reference value 0.270 – 4.200 mIU/L); QOL, quality of life; HDRS, Hamilton Depression Rating Scale; HARS, Hamilton Anxiety Rating Scale; MMSE, Mini-Mental State Examination; TAO, thyroid-associated ophthalmopathy; HC, healthy control, y, year; F, female; M, male; mo, month.

with a 20-channel head and neck coil. Magnetization-prepared rapid gradient echo sequence was used to acquire high-resolution 3D T1-weighted sagittal images. The parameters were as follows: echo time (TE) = 2.45 ms; repetition time (TR) = 1900 ms; flip angle = 9 degrees; voxel size = $1 \times 1 \times 1$ mm^3; field of view (FOV) = 256×256 mm^2; matrix size = 256×256; slice thickness = 1 mm; 176 slices. A spin echo planar diffusion sequence was applied to obtained DTI data with the following parameters: TE = 95 ms, TR = 10,000 ms, FOV = 256×256 mm^2, voxel size = $2 \times 2 \times 2$ mm^3, matrix size = 128×128, slice thickness = 2 mm without gap. Thirty sampling directions were acquired with a b factor of 1000 s/mm^2 after an acquisition without diffusion weighting (b = 0 s/mm^2) for reference.

Data Preprocessing and Network Construction

The DTI data were preprocessed using the Pipeline for Analyzing braiN Difusion imAges (PANDA) toolbox (http://www.nitrc.org/projects/panda) with the following steps. First, a binary brain mask was obtained from respective b = 0 images and the nonbrain tissues were removed. Second, effects of head motion and eddy current distortions were corrected using affine transformation to the b = 0 images.[22] Afterward, diffusion tensor eigenvalues and eigenvectors were estimated and fractional anisotropy was calculated.

The Anatomical Automatic Labeling (AAL) parcellation scheme was applied to divide each brain into 90 regions (45 in each hemisphere).[23] Each region was defined as one node and the interconnections between regions were taken as the edges of the structural network. The parcellation process were as follows: first, a linear transformation was used to register the preprocessed diffusion image of each subject to the corresponding T1-weighted images. Second, the individual transformed T1-weighted images were nonlinearly transformed to the ICBM125 (Montreal Neurological Institute [MNI]). Finally, the subject-specific inverse transfor-
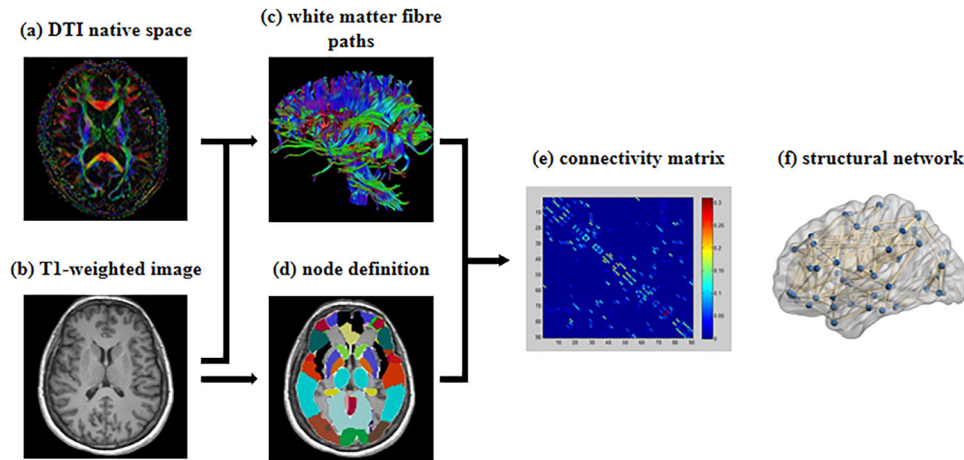
Figure 1. Flow chart for the construction of structural networks based on diffusion tensor imaging (DTI) data. (1) The DTI native space (**a**) was registered to the corresponding T1-weighted images (**b**) using a linear transformation. Then, the transformed T1-weighted image was nonlinearly transformed to the ICBM125 template in Montreal Neurological Institute (MNI) space. (2) The subject-specific inverse transformation was applied to transform Anatomical Automatic Labeling atlas from MNI space to the DTI native space (**d**). (3) A probabilistic fiber tracking approach was applied to reconstruct fiber paths (**c**). (4) A symmetric network matrix (**e**) for each subject was constructed and brain structural network (**f**) was obtained.

Table 2. Description of the Graph Network Parameters

Parameter	Description
Global network properties	
Shortest path length (Lp)	The average of the shortest path length for all possible edges among nodes in the network
Clustering coefficient (Cp)	The average likelihood that the neighbors of a node were interconnected
Small-worldness (σ)	$\sigma = Cp/Lp$; quantifies the organization of a network, with $\sigma > 1$ indicating a network has a mall-world property
Global efficiency (Eg)	Average inverse shortest path length, which measures the ability of parallel information transmission over the network
Local efficiency (Eloc)	Mean of the global efficiency of subgraphs computed on the immediate neighbors of a region, which is a measure of the fault tolerance of the network
Nodal network properties	
Nodal betweenness	The number of shortest paths in the network that run through a given node, which quantifies how much information may traverse the node
Nodal degree	A count of the number of connections that a node has to the other nodes in the network
Nodal efficiency	The average of inverse shortest path length between the node and the other nodes

mations were applied to warp the AAL atlas from the MNI space to the DTI native space. Then, a probabilistic streamline fiber tracking algorithm was applied to reconstruct fiber paths. In this way, a symmetric 90 × 90 network matrix for each subject was constructed and the brain structural network was obtained. The flow chart for construction of structural networks is shown in Figure 1.

Network Analysis

Graph theoretical properties were calculated to quantitatively clarify brain structural network topology characteristics. We calculated the global network topological properties with the following parameters: shortest path length (Lp), clustering coefficient (Cp), small-worldness (σ), global efficiency (Eg), and local efficiency (Eloc). Besides nodal betweenness, nodal degree and nodal efficiency were calculated to characterize the nodal properties of the brain. All the network metrics were computed using GRETNA toolbox on Matlab 2013b (MathWorks, Natick, MA, USA).[24] Table 2

gives a brief description of the abovementioned parameters.

Appropriate network thresholding is needed to create an equal number of nodes and connections across participants.[25] We examined the topological properties over a range of threshold ($0.06 \leq$ sparsity ≤ 0.43, step $= 0.01$) with the following criteria: (i) the structural network was sparce but fully connected; (ii) the average number of connections each node was larger than log of the total number of nodes; and (iii), the small-worldness of each brain network was > 1.2.[26] We further computed the area under the curve across the full range of the sparsity for comparison of global and nodal parameters. The value provides a summarized scale for the network topological properties, which makes it more sensitive to topologic alterations.[27]

Statistical Analysis

Between-group differences of demographic and clinical variables were tested using Student's *t* tests, Mann-Whitney *U* tests, and χ^2 tests. All tests were two-tailed and

significance was set at $P < 0.05$. These statistical analyses were performed using SPSS version 25.0 (SPSS, Chicago, IL, USA).

The alterations of network topological properties (Lp, Cp, σ, Eg, Eloc, nodal betweenness, nodal degree, and nodal efficiency) between patients with TAO and HCs were determined using two sample *t*-test with age, gender, and years of education as covariates (Bonferroni corrected, $P < 0.05$).

To localize the specific pairs of regions with altered structural connections in the TAO group, a network-based statistics (NBS) method was used.[28] First, the edge-by-edge comparison of the strength of edge weight in the structural connectivity matrix was conducted between patients with TAO and HCs using the two sample *t*-test. Second, the components that contained connected suprathreshold edges with P value of 0.001 were retained. Then, an empirical distribution of the connected component size was derived and the largest component size was calculated by repeating the abovementioned steps with 10,000 permutations and setting the P value at 0.05 corrected for multiple comparison. Before the permutation test, the effects of age, gender, and years of education were eliminated by multiple linear regression.

In patients with TAO, for network properties that showed significant between-group alterations, partial correlation analyses were performed to assess the relationships with disease duration, visual acuity, neuropsychiatric measurements, and serum thyroid function indexes with age, gender, and years of education as covariates. All correlation analyses were conducted with SPSS version 25.0 and the statistical threshold was set at $P < 0.05$.

RESULTS

Group Differences in Demographic and Clinical Data

Demographic and clinical information of participants are summarized in Table 1. Patients with TAO and HCs showed no significant between-group differences in age ($P > 0.999$), gender ($P > 0.999$), or education ($P = 0.881$). The average disease duration for TAOs was 24.0 ± 39.0 months and the mean CAS was 2.4 ± 1.4. The visual acuity values were significantly lower ($P = 0.038$) in patients with TAO than in HCs. The average QOL scores for visual functioning and appearance in the TAO group were 60.8 ± 30.7 and 57.5 ± 20.7, respectively. Patients with TAO had significantly higher HDRS ($P < 0.001$) and HARS ($P < 0.001$) scores, whereas lower MMSE ($P < 0.001$) scores than the HCs.

Global and Nodal Network Topology Analysis

There were no significant differences for all global network parameters between patients with TAO and HCs. Details about the comparison of global network parameters are shown in Supplementary Figure S1, Table S1, and Table S2. Compared with HCs, patients with TAO showed decreased nodal betweenness in right anterior cingulate and paracingulate gyri (ACG). Moreover, patients with TAO exhibited decreased nodal degree in the right orbital part of middle frontal gyrus (ORBmid) and right ACG, whereas they had increased nodal degree in the left cuneus. Reduced nodal efficiency in the right ORBmid and increased value in the left cuneus were also observed. The alterations of nodal network

TABLE 3. Brain Regions With Significant Changes in Nodal Network Parameters Between Patients With TAO and Controls ($P < 0.05$, Bonferroni Corrected)

Region	TAO	HC	T	P Value
Nodal betweenness				
ACG.R	7.046 ± 2.141	9.175 ± 2.193	-3.766	0.0004
Nodal degree				
ORBmid.R	3.930 ± 0.798	4.723 ± 0.736	-3.757	0.0005
ACG.R	6.859 ± 0.779	7.580 ± 0.608	-3.829	0.0004
CUN.L	5.799 ± 1.036	4.866 ± 0.748	3.787	0.0004
Nodal efficiency				
ORBmid.R	0.186 ± 0.006	0.192 ± 0.006	-3.919	0.0003
CUN.L	0.198 ± 0.009	0.190 ± 0.007	3.712	0.0005

Note: Data are presented as means $\pm$ standard deviations.

The values of nodal network parameters are indexed by area under the curve value.

R, right; L, left; ACG, anterior cingulate and paracingulate gyri; ORBmid, orbital part of middle frontal gyrus; CUN, cuneus; TAO, thyroid-associated ophthalmopathy; HC, healthy control.

properties between patients with TAO and HCs are exhibited in Table 3 and Figure 2.

### Altered Structural Network Connectivity in TAO

We identified one connected component with decreased structural connectivity strength in patients with TAO. The component consisted of right ORBmid, right putamen, left caudate nucleus, and left medial superior frontal gyrus (SFGmed). The results are presented in Figure 3. It is worth mentioning that the right ORBmid was identified as the core of this connected component.

Correlation Analysis

In patients with TAO, nodal degree in the right ORBmid and right ACG as well as nodal efficiency in the right ORBmid were negatively correlated with HARS ($r = -0.424$, $P = 0.039$; $r = -0.559$, $P = 0.005$; and $r = -0.438$, $P = 0.032$, respectively; Figs. 4a–c). Similarly, a negative relationship between nodal degree in the right ACG and HDRS was observed ($r = -0.470$, $P = 0.020$; Fig. 4d). Meanwhile, both nodal degree and nodal efficiency in left cuneus were negatively correlated with visual acuity ($r = -0.408$, $P = 0.048$; and $r = -0.420$, $P = 0.041$, respectively; Figs. 4e, 4f). No significant associations were found between the network properties and other clinical variables ($P > 0.05$).

DISCUSSION

It was the first study focused on the structural network topological alterations of patients with TAO by using DTI with graph theory. Our study had four major findings: (1) there were no alterations of global parameters in patients with TAO. (2) The nodal properties decreased in the right ACG and ORBmid, whereas they increased in the left cuneus in patients with TAO. (3) Decreased structural connections were found in the patient group involving the right ORBmid, right putamen, left caudate nucleus, and left SFGmed. (4) The altered nodal parameters were correlated with neuropsychological performances and visual acuity. These findings provided neuropsychiatric evidence for better
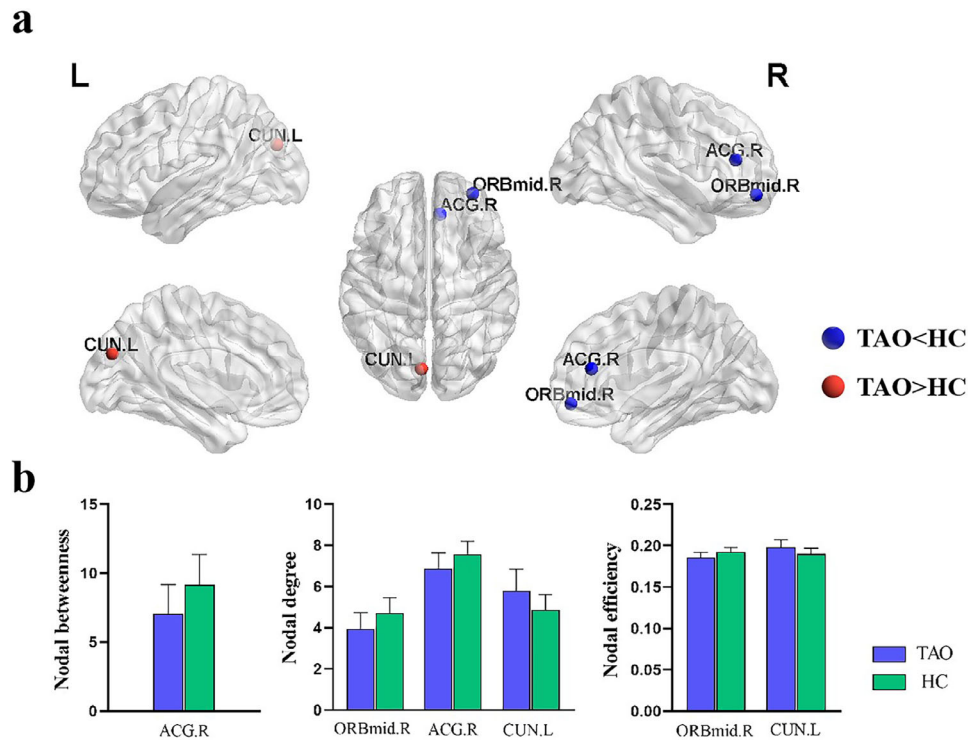
FIGURE 2. (a) Brain regions with significant changes in nodal network parameters between patients with TAO and controls ($P < 0.05$, Bonferroni corrected). (b) Between-group differences in nodal network parameters (indexed by area under the curve value). R, right; L, left; ACG, anterior cingulate and paracingulate gyri; ORBmid, orbital part of middle frontal gyrus; CUN, cuneus; TAO, thyroid-associated ophthalmopathy; HC, healthy control.
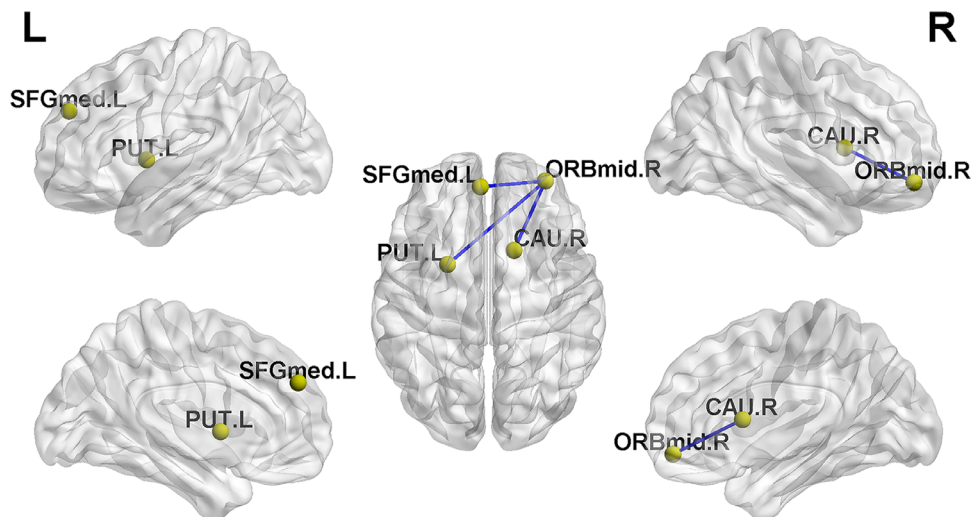

FIGURE 3. Decreased region-to-region structural connections obtained by network-based statistics ($P < 0.05$). R, right; L, left; ORBmid, orbital part of middle frontal gyrus; SFGmed, medial superior frontal gyrus; PUT, putamen of lenticular nucleus; CAU, caudate nucleus.

interpreting related clinical symptoms and extended our understanding of the disease.

The human brain network has been proven to hold small-worldness property constructed by various imaging modes.[29,30] Small-world network is a highly integrated and optimized network model that enables high efficiency in processing and transmission of information.[31] In this study, the structural brain networks of both patients with TAO and HCs distinctly exhibited small-world organiza-

tion. Moreover, no significant between-group differences on global network parameters were found. To the best of our knowledge, neuroimaging with graph theory has only been applied in the evaluation of patients with glaucoma in the field of ophthalmic disorders.[32] Similarly, they also found no disruption of global measures and preserved small-world property in patients with glaucoma, hinting that the efficiency of communication in the brain network was conserved and the brain was homogeneously well
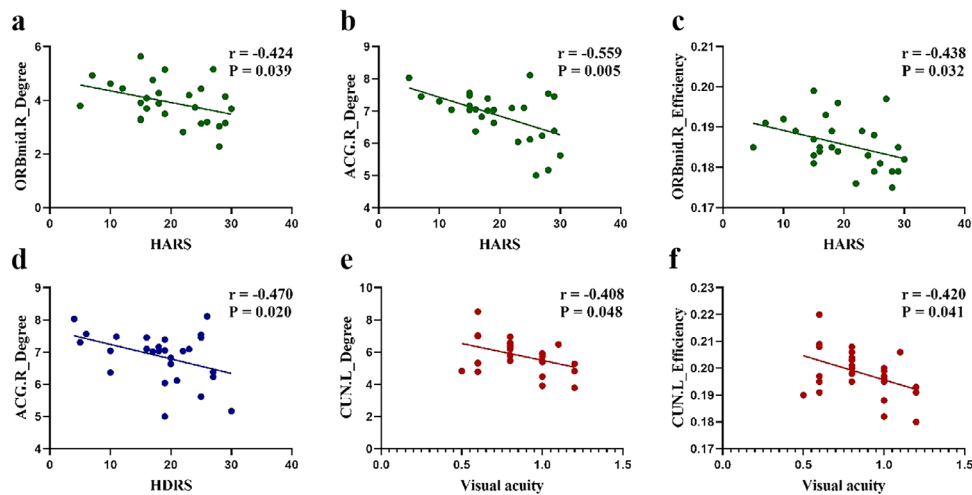
FIGURE 4. Correlation analyses results between structural network parameters and clinical characteristics. R, right; L, left; ACG, anterior cingulate and paracingulate gyri; ORBmid, orbital part of middle frontal gyrus; CUN, cuneus; HDRS, Hamilton Depression Rating Scale; HARS, Hamilton Anxiety Rating Scale.

re-organized.[32–34] Thus, in accord with their results, our current findings also indicated that the global structural connection was maintained and the overall ability of information processing was preserved in patients with TAO.

In contrast to the global topological findings, the nodal network parameters were discovered to change significantly in patients with TAO. Nodal betweenness measures the importance of a node in network communication, whereas nodal degree and nodal efficiency reflect the capacity of information integration and transmission.[35,36] A region with reduction of these nodal parameters indicates disruption of interconnectivity with other regions in the network. In this study, reduced nodal betweenness and nodal degree were observed in the right ACG. The cingulate gyrus, as the core node of default mode network, plays a critical role in transmission and integration of information.[31] Accumulated neuroimaging evidence has indicated that the anterior cingulate cortex was involved in emotional regulation, cognitive processes, and specific motor functions.[11,37,38] Previously, Silkiss et al. found thinning of the grey matter sheet in the right anterior cingulate and they linked it to the emotional disturbances in TAO.[11] Similarly, we also found decreased nodal properties in the right anterior cingulate, and negative correlations were observed between nodal degree in the right ACG and HARS as well as HDRS scores. Our results suggested that the decreased nodal topological properties in ACG may be related to impaired emotional regulation in TAO.

Meanwhile, decreased nodal degree and nodal efficiency in the right ORBmid were observed. The ORBmid lies in the orbitofrontal cortex (OFC), which is functioned in mood regulation and management of interpersonal relationships and social behaviour.[39,40] Decreased activity in the OFC has been observed in various anxiety-related disorders.[41,42] A previous resting-state functional MRI study found decreased activity of the right ORBmid in patients with anxious depression, speculating this region to be responsible for mood regulation and suicidal tendency.[40] In our study, the NBS analyses identified a subnetwork with decreased structural connections in the TAO cohort. All connections in the subnetwork involved the right ORBmid, highlighting the core role of this node in the disrupted structural network.

Our findings reflected the dysfunction of ORBmid in integrating and processing information in patients with TAO. In addition, Hornak et al. reported that patients with lesions in the OFC and anterior cingulate cortex had deficits in identifying signal from facial and voice expression and impairments in social behaviour.[43,44] As we know, most patients with TAO have difficulties in social relationships because of their ocular symptoms and complain of social isolation.[45] It was deemed that patients with TAO showed more remarkable anxiety and depression than patients with other chronic diseases or facial disfigurements.[46] Taken together, the decreased nodal parameters in the right ACG and ORBmid may be associated with the frequently presented affective symptoms in TAOs, which was further validated by the negative correlations with psychometric test scores.

Another important finding was the increased nodal degree and nodal efficiency in left cuneus. It is widely accepted that the cuneus is involved in visual processing and it is responsible for spatial location.[47,48] A previous study using traditional DTI indices has identified decreased fractional anisotropy and increased diffusivities in right cuneus, indicating the disturbance of visual processing in TAO.[10] In this study, the cuneus was found to exhibit increased nodal properties on the contrarily left hemisphere. Thus, we speculated that the increased nodal properties in the left cuneus may act as a compensatory mechanism to maintain the visual processing capacity to some extent. Besides, the negative correlations between nodal topological properties in the left cuneus and visual acuity suggested that the increased regional connectivity in the left cuneus was associated with impaired visual function, which was in line with our "compensatory" hypothesis.

Our results verified the existence of structural network alterations and the correlation between network topological properties and clinical-psychiatric conditions in patients with TAO. Understanding the neural patterns underpinning clinical appearances help clinicians to treat patients with TAO more comprehensively. Our study provided a visual presentation of structural brain connectome changes in TAO, which was more objective and intuitional to clinicians. In particular, antipsychotic medication or psychiatric services could be considered in the treatment plans when emotional

disturbances are being detected, thus improve patients' overall quality of life (QOL).

Several limitations in the present study need to be taken into consideration. First, the sample size of our study was relatively small. A greater number of subjects would yield more robust results. Second, a DTI sequence with 30 diffusion-encoding gradient directions was used in the current study. Application of advanced acquisitions with more diffusion directions could facilitate more detailed fiber tracking. Third, an atlas with 90 brain regions was used in the current study, which did not contain the cerebellum. The status of cerebellum in TAO investigated in further studies might yield more significance. Finally, we only enrolled the hematologically quiescent TAO subjects after antithyroid drugs therapy in order to minimize the influence of thyroid hormone. It is unknown whether the drugs therapy would have certain impact on the structural network in patients with TAO. Future studies comparing between subgroups (e.g. untreated patients with hyperthyroid versus treated patients with hyperthyroid with ophthalmopathy versus treated patients with hyperthyroid without ophthalmopathy) would confirm our results.

In conclusion, we used DTI incorporated with graph theoretical approach to examine the topological alterations of structural network in patients with TAO. Our results suggested that the disruption of network regions and connectivities was related to the clinical-psychiatric dysfunctions of patients with TAO.

References

1. Wiersinga WM, Prummel MF. Pathogenesis of Graves' ophthalmopathy–current understanding. *J Clin Endocrinol Metab*. 2001;86(2):501–503.
2. Muller-Forell W, Kahaly GJ. Neuroimaging of Graves' orbitopathy. *Best Pract Res Clin Endocrinol Meta*. 2012;26(3):259–271.
3. Bruscolini A, Sacchetti M, La Cava M, et al. Quality of life and neuropsychiatric disorders in patients with Graves' orbitopathy: current concepts. *Autoimmun Rev*. 2018;17(7):639–643.
4. Bahn RS. Graves' ophthalmopathy. *N Engl J Med*. 2010;362(8):726–738.
5. Coulter I, Frewin S, Krassas GE, Perros P. Psychological implications of Graves' orbitopathy. *Eur J Endocrinol*. 2007;157(2):127–131.
6. Edmunds MR, Huntbach JA, Durrani OM. Are ethnicity, social grade, and social deprivation associated with severity of thyroid-associated ophthalmopathy? *Ophthalmic Plast Reconstr Surg*. 2014;30(3):241–245.
7. Kahaly GJ, Petrak F, Hardt J, Pitz S, Egle UT. Psychosocial morbidity of Graves' orbitopathy. *Clin Endocrinol (Oxf)*. 2005;63(4):395–402.
8. Schlote B, Nowotny B, Schaaf L, et al. Subclinical hyperthyroidism: physical and mental state of patients. *Eur Arch Psychiatry Clin Neurosci*. 1992;24(6):357–364.
9. Demet MM, Ozmen B, Deveci A, Boyvada S, Adiguzel H, Aydemir O. Depression and anxiety in hyperthyroidism. *Arch Med Res*. 2002;33(6):552–556.
10. Wu Q, Hu H, Chen W, et al. Morphological and microstructural brain changes in thyroid-associated ophthalmopathy: a combined voxel-based morphometry and diffusion tensor imaging study. *J Endocrinol Invest*. 2020;43(11):1591–1598.
11. Silkiss RZ, Wade AR. Neuroanatomic variations in Graves' dysthyroid ophthalmopathy as studied with MRI. *Trans Am Ophthalmol Soc*. 2016;114:T9.
12. Friston KJ. The disconnection hypothesis. *Schizophr Res*. 1998;30(2):115–125.
13. Rubinov M, Sporns O. Complex network measures of brain connectivity: uses and interpretations. *Neuroimage*. 2010;52(3):1059–1069.
14. Sporns O. Graph theory methods: applications in brain networks. *Dialogues Clin Neurosci*. 2018;20(2):111–121.
15. Gleichgerrcht E, Kocher M, Bonilha L. Connectomics and graph theory analyses: novel insights into network abnormalities in epilepsy. *Epilepsia*. 2015;56(11):1660–1668.
16. Jones DK, Griffin LD, Alexander DC, et al. Spatial normalization and averaging of diffusion tensor MRI data sets. *Neuroimage*. 2002;17(2):592–617.
17. Zobel A, Joe A, Freymann N, et al. Changes in regional cerebral blood flow by therapeutic vagus nerve stimulation in depression: an exploratory approach. *Psychiatry Res*. 2005;139(3):165–179.
18. Wang L, Bi K, An J, et al. Abnormal structural brain network and hemisphere-specific changes in bulimia nervosa. *Transl Psychiatry*. 2019;9(1):206.
19. Cho EB, Han CE, Seo SW, et al. White matter network disruption and cognitive dysfunction in neuromyelitis optica spectrum disorder. *Front Neurol*. 2018;9:1104.
20. Wang B, Li T, Zhou M. The abnormality of topological asymmetry in hemispheric brain anatomical networks in bipolar disorder. *Front Neurosci*. 2018;12:618.
21. Bartalena L, Baldeschi L, Boboridis K. The 2016 European Thyroid Association/European Group on Graves' Orbitopathy Guidelines for the Management of Graves' Orbitopathy. *Eur Thyroid J*. 2016;5(1):9–26.
22. Jenkinson M, Bannister P, Brady M, Smith S. Improved optimization for the robust and accurate linear registration and motion correction of brain images. *Neuroimage*. 2002;17(2):825–841.
23. Tzourio-Mazoyer N, Landeau B, Papathanassiou D. Automated anatomical labeling of activations in SPM using a macroscopic anatomical parcellation of the MNI MRI single-subject brain. *Neuroimage*. 2002;15(1):273–289.
24. Wang J, Wang X, Xia M, Liao X, Evans A, He Y. GRETNA: a graph theoretical network analysis toolbox for imaging connectomics. *Front Hum Neurosci*. 2015;9:386.
25. Korgaonkar MS, Fornito A, Williams LM, Grieve SM. Abnormal structural networks characterize major depressive disorder: a connectome analysis. *Biol Psychiatry*. 2014;76(7):567–574.
26. Wang J, Khosrowabadi R, Ng KK, et al. Alterations in brain network topology and structural-functional connectome coupling relate to cognitive impairment. *Front Aging Neurosci*. 2018;10:404.
27. Wang YF, Gu P, Zhang J. Deteriorated functional and structural brain networks and normally appearing functional-structural coupling in diabetic kidney disease: a graph theory-based magnetic resonance imaging study. *Eur Radiol*. 2019;29(10):5577–5589.
28. Zalesky A, Fornito A, Bullmore ET. Network-based statistic: identifying differences in brain networks. *Neuroimage*. 2010;53(4):1197–1207.

29. Achard S, Salvador R, Whitcher B, Suckling J, Bullmore E. A resilient, low-frequency, small-world human brain functional network with highly connected association cortical hubs. *J Neurosci*. 2006;26(1):63–72.

30. He Y, Chen ZJ, Evans AC. Small-world anatomical networks in the human brain revealed by cortical thickness from MRI. *Cereb Cortex*. 2007;17(10):2407–2419.

31. Golchert J, Smallwood J, Jefferies E, et al. In need of constraint: understanding the role of the cingulate cortex in the impulsive mind. *Neuroimage*. 2017;146:804–813.

32. Wang J, Li T, Wang N, Xian J, He H. Graph theoretical analysis reveals the reorganization of the brain network pattern in primary open angle glaucoma patients. *Eur Radiol*. 2016;26(11):3957–3967.

33. Minosse S, Garaci F, Martucci A, et al. Primary open angle glaucoma is associated with functional brain network reorganization. *Front Neurol*. 2019;10:1134.

34. Nucci C, Garaci F, Altobelli S, et al. Diffusional kurtosis imaging of white matter degeneration in glaucoma. *J Clin Med*. 2020;9(10):3122.

35. Qin C, Liang Y, Tan X, et al. Altered whole-brain functional topological organization and cognitive function in type 2 diabetes mellitus patients. *Front Neurol*. 2019;10:599.

36. Shu N, Wang X, Bi Q, Zhao T, Han Y. Disrupted topologic efficiency of white matter structural connectome in individuals with subjective cognitive decline. *Radiology*. 2018;286(1):229–238.

37. Lan DY, Zhu PW, He Y, et al. Gray matter volume changes in patients with acute eye pain: a voxel-based morphometry study. *Transl Vis Sci Technol*. 2019;8(1):1.

38. Zhang W, Liu X, Zhang Y. Disrupted functional connectivity of the hippocampus in patients with hyperthyroidism: evidence from resting-state fMRI. *Eur J Radiol*. 2014;83(10):1907–1913.

39. Greene JD, Sommerville RB, Nystrom LE, Darley JM, Cohen JD. An fMRI investigation of emotional engagement in moral judgment. *Science*. 2001;293(5537):2105–2108.

40. Zhao P, Yan R, Wang X. Reduced resting state neural activity in the right orbital part of middle frontal gyrus in anxious depression. *Front Psychiatry*. 2019;10:994.

41. Hahn A, Stein P, Windischberger C. Reduced resting-state functional connectivity between amygdala and orbitofrontal cortex in social anxiety disorder. *Neuroimage*. 2011;56(3):881–889.

42. Lorberbaum JP, Kose S, Johnson MR. Neural correlates of speech anticipatory anxiety in generalized social phobia. *Neuroreport*. 2004;15(18):2701–2705.

43. Hornak J, Bramham J, Rolls ET. Changes in emotion after circumscribed surgical lesions of the orbitofrontal and cingulate cortices. *Brain*. 2003;126(Pt 7):1691–1712.

44. Hornak J, Rolls ET, Wade D. Face and voice expression identification in patients with emotional and behavioural changes following ventral frontal lobe damage. *Neuropsychologia*. 1996;34(4):247–261.

45. Jensen AL, Harder I. The impact of bodily change on social behaviour in patients with thyroid-associated ophthalmopathy. *Scand J Caring Sci*. 2011;25(2):341–349.

46. Wickwar S, McBain HB, Ezra DG, Hirani SP, Rose GE, Newman SP. Which factors are associated with quality of life in patients with Graves' orbitopathy presenting for orbital decompression surgery? *Eye (Lond)*. 2015;29(7):951–957.

47. Rosen ML, Sheridan MA, Sambrook KA, Peverill MR, Meltzoff AN, McLaughlin KA. The role of visual association cortex in associative memory formation across development. *J Cogn Neurosci*. 2018;30(3):365–380.

48. Zhu PW, Huang X, Ye L. Altered intrinsic functional connectivity of the primary visual cortex in youth patients with comitant exotropia: a resting state fMRI study. *Int J Ophthalmol*. 2018;11(4):668–673.